

**Modulation of neuronal network activity using magnetic nanoparticle-based astrocytic network integration**

Journal:	<i>Biomaterials Science</i>
Manuscript ID:	BM-ART-03-2015-000092.R1
Article Type:	Paper
Date Submitted by the Author:	17-May-2015
Complete List of Authors:	Saito, Atsushi; Central Research Institute of Electric Power Industry, Environmental Science Research Laboratory Nakashima, Yutaro; The University of Tokyo, Graduate School of Frontier Sciences Shimba, Kenta; The University of Tokyo, Graduate School of Frontier Sciences Takayama, Yuzo; National Institute of Advanced Industrial Science and Technology (AIST), Biotechnology Research Institute for Drug Discovery Kotani, Kiyoshi; The University of Tokyo, Graduate School of Engineering Jimbo, Yasuhiko; The University of Tokyo, Graduate School of Engineering

### Title

Modulation of neuronal network activity using magnetic nanoparticle-based astrocytic network integration

### Authors

Atsushi Saito<sup>a1</sup>, Yutaro Nakashima<sup>b2</sup>, Kenta Shimba<sup>b2</sup>, Yuzo Takayama<sup>c3</sup>, Kiyoshi Kotani<sup>d4</sup>, and Yasuhiko Jimbo<sup>d4</sup>

### Affiliation

<sup>a1</sup> Environmental Science Research Laboratory, Central Research Institute of Electric Power Industry (CRIEPI)

<sup>b2</sup> Graduate School of Frontier Sciences, The University of Tokyo

<sup>c3</sup> [Biotechnology Research Institute for Drug Discovery, National Institute of Advanced Industrial Science and Technology \(AIST\)](#)~~Research Center for Stem Cell Engineering, National Institute of Advanced Industrial Science and Technology (AIST)~~

<sup>d4</sup> Graduate School of Engineering, The University of Tokyo

### Abstract

Investigating the mechanisms of neuron-glia interaction is important in basic research of neuroscience and neural transplantation. Synaptic transmission is modulated by astrocyte activations in the pre- and post-synaptic terminals, and this phenomenon is spread to the surrounding astrocytes through gap junctions. However, the modulation of network-wide neuronal activity dependent on extensive astrocyte activation is not well understood. In this study, we show network-wide neuronal modulation associated with a newly developed three-dimensional neuronal and astrocytic network co-culture method. To establish widespread neuronal and astrocytic network interactions *in vitro*, we performed integration of magnetic nanoparticle-injected astrocytes (Mag-AS) on the matured monolayer of neuronal networks using external magnetic force. The neuronal electrical activity was dynamically synchronized at 24 h after integration of Mag-AS network. Additionally, Mag-AS network activation using a caged calcium compound rapidly induced suppression and subsequent synchronization of neuronal electrical activity. These results indicate that the high-density astrocytic network integration onto the neuronal network can induce ~~the~~-widespread neuronal modulation, and our *in vitro* ~~3D~~-co-culture method contributes to advancement of neuronal and astrocytic transplantation research.

### Keywords

Neuron-glia interaction, neuronal network, astrocyte, magnetic nanoparticles, microelectrode array

## 1.1 Introduction

In order to understand the mechanisms of cell-to-cell interactions after neural transplantation within complex brain functions, the development of a simplified method is important for investigating the effects of transplanted cells on neuronal network function. The analysis of electrical activity using microelectrode array (MEA) is a promising method to evaluate cell function within a network *in vitro*. Moreover, this method can be combined with pharmaceutical<sup>[1-5]</sup>, electrical<sup>[6-9]</sup>, magnetic<sup>[5, 10]</sup>, and optical stimulation<sup>[11]</sup> as well as micro-patterning tools<sup>[12-15]</sup>. On the other hand, these experiments have often used dissociated neurons, in which the extracellular matrix was degraded by proteolytic enzyme, and thus the ~~vertically-integrated three-dimensional~~ layered structure was lost in the *in vitro* neuronal network. Therefore, the ~~three-dimensional (3D)~~ reconstruction method ~~using~~ using a ~~bottom-up~~ approach of ~~a two-dimensional neuronal network and vertically-layered structure~~ on MEA is useful in the assessment of cell transplantation, disease mechanisms, and brain-like tissue.

Astrocytes are a group of glial cells that bear the important role of supporting a neuronal cells and supplying nutrients through the blood-brain barrier. More interestingly, astrocytic activity strongly modulates neuronal network activity through the regulation of synaptic transmission<sup>[16-23]</sup> and axonal conductance<sup>[24]</sup>. ~~it was also reported that this neuronal modulation is involved in epileptic seizures [25, 26].~~ In this process, gliotransmitters, such as adenosine triphosphate (ATP) and glutamate, are released when the astrocytes respond to the neuronal activity and ~~their~~ its excitation is spread to the surrounding astrocytes through gap junctions<sup>[16-23]</sup>. These mechanisms are not only involved in unilateral neuronal activation but also in mutual interaction within widespread neuronal networks. However, the systematic interaction between neuronal and astrocytic networks is unclear. ~~To observe this phenomenon, it is necessary that a physical joint structure be able to forming between each different network for efficient of the electric-chemical interaction.~~

In this study, we tried to establish a fundamental ~~vertically-layered 3D neuronal and astrocytic network~~ co-culture method to evaluate the direct interaction between neuronal and astrocytic networks. We magnetically integrated the astrocytes injected with magnetic nanoparticles (MNPs) onto the monolayer neuronal network and recorded the time-dependent changes of spontaneous electrical activity of the neuronal network by using MEA. Furthermore, we assessed the effects of astrocytic excitation on neuronal activity with a combination of optical stimulation using caged compounds and extracellular recordings. Based on these results, we present the main features of neuronal-astrocytic network interaction.

## 2. Experimental

### 2.1.2 Materials and Methods

Formatted: Font: Bold

Formatted: Superscript

Formatted: Superscript

Formatted: Superscript

Formatted: Superscript

Formatted: Superscript

Formatted: Font color: Red

Formatted: Font color: Red

Formatted: Font color: Red

Formatted: Superscript

Formatted: Superscript

Formatted: Superscript

Formatted: Superscript

Formatted: Font color: Red

Formatted: Font: Bold

Formatted: Font: Bold

## 2.1 Cell culture

All animal experiments were approved by the animal experiments ethics committee at the University of Tokyo and performed according to the University of Tokyo guidelines for the care and use of laboratory animals. We harvested the cells from cortical tissue, which is one of the astrocyte-rich brain regions. Isolation and culture of cortical neurons and astrocytes were performed using the following methods. Cortical tissue harvested from 18–19-day-old Wistar rat embryos was enzymatically dissociated into single cells with a 15–20 min treatment with 0.5% Trypsin solution (Sigma-Aldrich). Dulbecco's modified Eagle's medium (Invitrogen) containing 10% fetal bovine serum (Invitrogen), 5% horse serum (Invitrogen), and 1% penicillin-streptomycin (Pe-St) (Invitrogen) were used for the cell culture medium. The isolated neuronal and glial cells were seeded on the 0.1% polyethylenimine (PEI) coated MEA substrate with a density of  $3 \times 10^5$  cells/mm<sup>2</sup>. In addition, we locally cultivated the cells on the MEA area, and the monolayer network was smaller than 2-mm diameter in size. The plated monolayer networks were incubated at 37°C with a 5% CO<sub>2</sub> atmosphere and water vapor condition. During the incubation period, half of the medium was exchanged with fresh medium twice a week to maintain the culture conditions.

## 2.2 Magnetic nanoparticle injection in astrocytes and vertically-layered 3D co-culture

To control the interactions between neuronal networks and astrocytes artificially, cultured astrocytes were injected with MNPs (Mag-AS; MNP-injected astrocytes) and integrated with the cultured monolayer of neurons. The schematic diagram of the experiment is summarized in Figure 1. Considering the negative membrane potential of glial cells, we used cationic dispersed liposomes containing MNP (EMG607, FerroTech). The MNP have an average diameter of about 10-nm. The MNP core is a mixture of Fe<sub>3</sub>O<sub>4</sub> and gamma-Fe<sub>2</sub>O<sub>3</sub>, which are well known to be compatible with living body tissue. To promote the injection efficiency of MNP into astrocytes, we decreased the proportion of neuronal cells in a culture dish through frequent repetition of the subculture. Sub-confluent astrocytes in a 35-mm dish, which contained  $1 \times 10^6$  cells/cm<sup>2</sup>, were prepared for MNP injection experiments. MNPs were endocytosed into astrocytes by bulk loading. The concentration and duration of MNP treatment was 0.01–10 mg/mL and 24 h, respectively. To confirm the MNP injection into cells, we evaluated the cell form, magnetic susceptibility of cells response, and rate of cell death. Before Mag-AS integration, the monolayer neuronal and glial networks were cultivated for four weeks or more on the MEA. To cover the whole area (diameter < 2 mm) of monolayer network, which was locally cultivated on the MEA, we pulled the Mag-AS downward from the upper side of the culture medium by positioning a magnet (size 3×3 mm, magnetic flux density 500 mT) under the MEA. In addition, to form a strong attachment of the Mag-AS with the monolayer network, the magnetic-hold on the culture was maintained for 24 h overnight.

Formatted: Font: Bold

Formatted: Font: Bold, Font color: Red

Formatted: Font: Bold

Formatted: Font color: Red

Formatted: Font color: Red

Formatted: Font color: Red

Formatted: Font color: Red

Formatted: Font color: Red

Formatted: Font color: Red

Formatted: Font color: Red

Formatted: Font color: Text 1

Formatted: Font color: Red

Formatted: Font color: Red

### 2.3 Evaluation of neuronal network activity

To evaluate the effects of the integration of astrocytic networks on the neuronal activity, we monitored network-wide electrical activity using the MEA-based extracellular recording system. The square array of 64 electrodes in the centre of the MEA substrate permitted multi-point, wide-area, and long-term recording of spontaneous electrical activity during neuronal network development. The 30×30 μm square electrodes of MEA were arranged in an 8×8 matrix with a 180 μm separation between electrodes. The extracellular signals from these electrodes were amplified 10,000 times with pre- and post-amplifiers (NF Co.), filtered using a 100–2,000 Hz band-pass filter (NF Co.), A/D converted at a 25 kHz sampling rate using LabVIEW software (National Instruments), and stored on a hard disk. The recorded data were visualized by PV-wave software (Visual Numerics), and the spikes were detected by a previously published method.<sup>51</sup> In our experiments, the maturation of neuronal network activity was defined as the stability of spontaneous activity, synchronized burst intervals, and morphological changes on the MEA substrate. Statistical analysis of the recorded data was performed by Student's t-test.

Formatted: Font: Bold

Formatted: Superscript

### 2.4 Optical and pharmaceutical induction and observation of calcium transients in Mag-AS

A caged calcium compound (NP-EGTA AM, Molecular Probes) and adenosine triphosphate (ATP) solution (ATP solution, Life Technologies) were used in order to increase intracellular Ca<sup>2+</sup> concentration in Mag-AS at arbitrary time points. Mag-AS activity was optically measured by using a fluorescent probe for calcium imaging (Fluo-4 AM, Molecular Probes). Release of Ca<sup>2+</sup> from the NP-EGTA AM was achieved with ultra-violet (UV) light irradiation from a light-emitting diode (LED) arranged over the MEA. The concentrations of Fluo-4 AM and NP-EGTA AM were 10 μM, and these agents were penetrated to the cells over 30 min in a CO<sub>2</sub> incubator. The concentration of ATP solution was 1 μM and which was bath-applied to the bath during fluorescent imaging of calcium activity of astrocytes. The fluorescence images were acquired at 500 ms/frame by a cooled charge-coupled device (CCD) camera (C8800-21C, Hamamatsu Photonics) and the HiPic7 software (Hamamatsu Photonics). The luminance values acquired from the recorded data were analysed using PV-WAVE (Visual Numerics).

Formatted: Font: Bold

Formatted: Font: Bold, Font color: Red

Formatted: Font: Bold

Formatted: Font: Bold, Font color: Red

Formatted: Font: Bold

Formatted: Font color: Red

Formatted: Font color: Red

Formatted: Font color: Red

Formatted: Font color: Red

### 2.5 Immunohistochemistry

Neuronal cell death and increase in population of astrocytes accompanying the subculture were evaluated by immunohistochemical analysis. The samples were fixed with 4% paraformaldehyde for 20 min at room temperature. After washing in phosphate buffered saline (PBS) (1 min × 3), the fixed cells were permeabilized with 0.25% TritonX-100 in PBS for 10 min and then blocked with 4% bovine serum albumin (BSA). For primary antibodies, we used mouse anti-beta-III

Formatted: Font: Bold

tubulin (anti-B3T, 1:400, Chemicon International) and rabbit anti-glial fibrillary acidic protein (anti-GFAP, 1:1000, Chemicon International). These antibodies were applied overnight at 4°C. On the next day, the samples were washed in PBS (5 min × 3) and incubated for 2 hours at room temperature with Alexa Fluor 488-mouse IgG (1:500, Molecular Probes) and Alexa Fluor 546-rabbit IgG (1:500, Molecular Probes). Immunochemical images were obtained with a cooled CCD camera combined with an inverted microscope (IX-71, Hamamatsu Photonics).

### 3 Results

#### 3.1 Preparing the MNP-injected astrocytes

To prepare a high-density astrocyte culture, we manipulated the number of subcultures to promote neuronal cell death. Statistical analysis using Student's t-test showed that the positive area for the neural marker B3T in cultured cells was significantly reduced (\*\* $P < 0.001$ ,  $n=4$ , error bars  $\pm$ SD), whereas the positive area for the astrocyte marker GFAP was unchanged after repetitions of subculture (Fig. 2A, and 2B). With this procedure, we confirmed that over 90% of the neural marker-positive area had disappeared with more than three times of subcultures. Next, to determine the concentrations of MNPs in the culture medium, we compared the additive concentration with magnetic force response and cell death. Subsequent to the injection of different concentrations (0.01–1 mg/mL), cultured astrocytes ( $5 \times 10^6$  cells in 35-mm Petri dish) were dispersed to single cells by trypsin treatment and used for transduction assay. Phase contrast images showed that the astrocytes were markedly covered with the MNPs at a concentration of 1 mg/mL after MNP injection (Fig. 2C). Here, cell morphology and number of cells before and after injection of MNP were nearly unchanged due to contact inhibition. Although the Mag-AS generally adhered to the magnet stand-attached cell culture dishes, occupancy of Mag-AS in the magnetized areas was correlated with concentration (Fig. 2DB and 2EC). In particular, the most effective concentration was 1 mg/mL which showed over 90% of Mag-AS attachment; the percentage of Mag-AS-covered area rose 2-fold with a 10-fold increase of MNP concentration (Fig. 2EC). Figure 2FD shows the result of statistical analysis using Student's t-test on the percentage of cell death after MNP injection and enzymatical cell detachment. The ratio of cell death remained unchanged at 1 mg/mL, however, the higher concentration (10 mg/mL) induced cell rupture (\*\* $P < 0.001$ ,  $n = 4$ , error bars  $\pm$ SD). Based on these results, we used the 1 mg/mL concentration for the final development of Mag-AS-integrated networks.

#### 3.2 Mag-AS induced changes in spontaneous electrical activity of the monolayer neuronal network

To confirm whether neuronal network activity was modulated by the Mag-AS formed astrocytic network integration, we compared time-dependent changes of spontaneous activity

Formatted: Font: Bold

Formatted: Font color: Red

Formatted: Font color: Red

Formatted: Font color: Red

Formatted: Font color: Red

Formatted: Font color: Red

Formatted: Font color: Red

Formatted: Font color: Red

Formatted: Font color: Red

Formatted: Font color: Red

Formatted: Font color: Red

Formatted: Font: Bold

recorded by a non-invasive multi-site recording system (Fig. 3A). Prior to starting the Mag-AS integration, neuronal and glial cells were conventionally cultured on the MEA. The assessment of functional maturation of neuronal networks was based on the spontaneous electrical activity patterns recorded from all 64 electrodes for two months. The seeding area of cells was smaller than the magnet size to ensure that the whole surface of the monolayer network was covered by Mag-AS. Although the spontaneous electrical activity patterns of the monolayer networks changed dynamically during two weeks, the number of spikes and bursting activity stabilized after four weeks. Therefore, we used the monolayer networks cultured for over four weeks and recorded spontaneous activity from almost all electrodes. Figure 3B shows the spontaneous activity of the MNP-injected monolayer neuronal network on the same electrode. We confirmed that the activity pattern was nearly unchanged during development and MNP injection.

Shortly after seeding Mag-AS into the monolayer sample, the Mag-AS were pulled rapidly to the magnet and aggregated on the monolayer networks (Fig. 3CB). The sample remained on the magnet stand up to 24 h overnight in the CO<sub>2</sub> incubator to form a robust cell-to-cell connection.

The time-dependent changes of spontaneous activity patterns were compared before and after the Mag-AS integration. Figure 3DC illustrates the spontaneous electrical activity of one of the Mag-AS-integrated cultures as recorded by MEA. Electrical signals (E1 to E3) from each culture stage (before, initial, after 2 and 24 h after integration of Mag-AS) were recorded from the same electrode in MEAs. Although the detected activities were similar at initial and 2 h after integration for each electrode and culture stage, there was a great divergence in bursting width and interval at 24 h after integration. Figure 3ED shows that number of spikes after 24 h of Mag-AS integration decreased by approximately 50% compared to the initial state (\**P* < 0.05, n = 6, error bars ±SD).

### **3.3 Effect of Mag-AS integration on bursting intervals of neuronal network**

The multi-site recording data serve as an index of the functional connection between neuronal and astrocytic networks. Mag-AS integrated networks induced rhythmic electrical activities such as periodic synchronized bursting patterns. Therefore, we compared the burst time interval between monolayer networks and Mag-AS-integrated networks (Fig. 4). In the monolayer networks, the average time interval for 10 times of successive bursting was 2.7–3.8 s (Fig. 4AB). In contrast, the average in the Mag-AS integrated network was 2.5–9.2 s (Fig. 4BC). Although the burst intervals of 10 s or longer were not seen in the monolayer network (Fig. 4C), ~~it~~ they were observed in three samples of the Mag-AS-integrated network. In particular, in the integrated networks, we observed “silent periods” with completely absent activity for over 20–30 s (Fig. 4D). Based on these experimental results, we confirmed that the Mag-AS-integrated astrocytic network adjusted neuronal activities at the network level as represented by the synchronized activity.

Formatted: Font color: Red

Formatted: Font color: Red

Formatted: Font color: Red

Formatted: Font color: Red

Formatted: Font color: Red

Formatted: Font color: Red

Formatted: Font color: Red

Formatted: Font color: Red

Formatted: Font color: Red

Formatted: Font color: Red

Formatted: Font color: Red

Formatted: Font color: Red

Formatted: Font color: Red

Formatted: Font: Bold

Formatted: Font color: Red

Formatted: Font color: Red

Formatted: Font color: Red

Formatted: Font color: Red

### 3.4 Modulation of neuronal network activity by induction of Mag-AS excitation

Gliotransmitters, such as ATP and glutamate, are discharged at the time of astrocyte excitation and accompanying intracellular calcium oscillation. To investigate the effects of the excitation of astrocytic networks on spontaneous bursting activity in the neuronal network, we carried out real-time recordings while artificially raising cellular calcium concentrations of the astrocytes contained in an integrated network. Here, the  $\text{Ca}^{2+}$  calcium transients of the integrated networks were controlled by using the caged calcium compound NP-EGTA AM and UV irradiation. Spontaneous and artificially-induced intracellular  $\text{Ca}^{2+}$  oscillations in Mag-AS are shown in Figure 5. The time-durations of propagated spontaneous  $\text{Ca}^{2+}$  transient oscillations were about 5–10 s (Fig. 5A). These wave-like  $\text{Ca}^{2+}$  transient oscillations spread widely through gap junctions of astrocytes; thus, the astrocytic connections were not affected by MNP injection. Moreover, Mag-AS responded to the ATP solution similar to the monolayer astrocytes (without MNP) (Fig. 5B). Figure 5C and 5DB shows that the UV-induced  $\text{Ca}^{2+}$  transient oscillations repeatedly imitated the spontaneously evoked oscillations in a localized region. However, the reproducible  $\text{Ca}^{2+}$  responses by periodic UV exposure differed depending on the number of exposure trials (Fig. 5C). Therefore, it is necessary to be careful with repeated excitations of Mag-AS for the evaluation of neuronal and astrocytic network interactions. Figure 5D shows the effects of UV exposure on caged calcium (NP-EGTA AM) in MNP-injected astrocytes. Although Mag-AS excitation was not seen with UV exposure only, a rapid and a simultaneous response with UV exposure was observed after application of caged calcium. Here, the intervals of UV-evoked  $\text{Ca}^{2+}$  transients were short compared with the spontaneously activated  $\text{Ca}^{2+}$  transients (it has few minutes interval) of astrocytes. Therefore, the spontaneous calcium transients were undetectable in the continuously activated astrocytes using caged calcium. These UV-responsive properties were similar in the monolayer astrocytes (without MNP). These results indicated that the response properties by caged calcium were not altered after MNP injection in astrocytes.

To observe the direct effects of the astrocytic activity on the neuronal activity, real-time recording of spontaneous bursts in the Mag-AS-integrated networks were performed with the release of caged calcium. Changes in burst time intervals of monolayer ( $n=3$ , over 4 weeks in culture) and integrated ( $n=3$ , over 4 weeks in culture and 12 hours after integration) networks are shown in Figure 6. Before the experiments, we confirmed that modulation of neuronal electrical activity was not induced by short-time UV exposure (data not shown). The individual traces and averaged results indicate that neuronal activity modulation occurred with the release of caged calcium. Although the frequency of synchronized bursting activity was completely abolished immediately after UV irradiation in the monolayer network (Fig. 6A and 6C), alternating silent periods and high-frequency patterns of bursting activities were generated in the Mag-AS-integrated networks (Fig. 6B and 6D).

Formatted: Font: Bold

Formatted: Superscript

Formatted: Superscript

Formatted: Font color: Red

Formatted: Font color: Red

Formatted: Font color: Red

Formatted: Font color: Red

Formatted: Font color: Red

Formatted: Font color: Red

Formatted: Font color: Red

Formatted: Font color: Red

Formatted: Font color: Red

Formatted: Font color: Red

Formatted: Font color: Red

Formatted: Font color: Red

Formatted: Font color: Red, Superscript

Formatted: Font color: Red

Formatted: Font color: Red

Formatted: Font color: Red, Superscript

Formatted: Font color: Red

Formatted: Font color: Red

Formatted: Font color: Red

Formatted: Font color: Red

Formatted: Font color: Red

Formatted: Font color: Red

Formatted: Font color: Red

Formatted: Font color: Red

Formatted: Font color: Red

Formatted: Font color: Red

Formatted: Font color: Red

Formatted: Font color: Red

Formatted: Font color: Red

Formatted: Font color: Red

Formatted: Font color: Red



In particular, the duration of the silent period in the integrated networks increased immediately after UV exposure (Fig. 6D). These results suggest that the induction of silent periods within neuronal networks by astrocyte activation participated in the generation of synchronized periodic bursting.

Formatted: Font color: Red

#### 4 Discussion

Formatted: Font: Bold

In the present study, we developed a magnetic force-based vertically-layered 3D co-culture method for studying neuron-astrocyte interaction and demonstrated the induction of synchronized bursting activity in neuronal networks by astrocytic  $\text{Ca}^{2+}$  release.

Formatted: Font color: Red

The ratio of astrocytes to neurons within the cerebral cortex is about 0.4 times in rat and about 2–3 times in human<sup>[27]</sup>. Therefore, we adjusted the addition of Mag-AS to achieve a ratio similar to human cortex. In addition, neuronal and astrocytic networks were blended by the MNPs and exposed to external magnetic fields in order to promote a rapid interaction of electrical and chemical signals. After the 24 h magnetic-hold culture, the Mag-AS network adhered strongly, and there was no cell detachment after magnet removal. In previous research, the intracellular electrical coupling in cardiac tissue formed in an analogous fashion was confirmed in MNP-injected cardiomyocytes<sup>[28]</sup>. Although electrical coupling was not seen in the gap junction of astrocytes, several experiments demonstrated that gap junctions contribute to the transmission of  $\text{Ca}^{2+}$  between astrocytes, and astrocyte  $\text{Ca}^{2+}$  release accompanied by the release of glutamate and ATP modulates neuronal synaptic transmission<sup>[16-23]</sup>. In our experimental results, the wave-like  $\text{Ca}^{2+}$  transients were observed in the Mag-AS network after integration on the monolayer network, and the synchronized bursting activities, which alternately produced suppression and excitation, were confirmed within 24 h of integration of Mag-AS. This phenomenon suggests that Mag-AS-derived neurohumoral factors affected widespread neuronal network activity. Other experiments also revealed that protein kinase C activation by the astrocyte attachment to the neuronal cells affected the number of excitable synapses and the modulation of neuronal network activity<sup>[29, 30]</sup>. Therefore, it is necessary to further consider the influence of cell adhesion on synapse formation.

Formatted: Superscript

Formatted: Superscript

Formatted: Superscript

Formatted: Superscript

Finally, we confirmed the periodic synchronized bursting activity in neuronal networks when intracellular  $\text{Ca}^{2+}$  of Mag-AS was released artificially using a caged calcium compound. Immediately after UV exposure, rapid  $\text{Ca}^{2+}$  changes occurred in Mag-AS within 2–5 s. This temporal property resembles spontaneously activated astrocyte  $\text{Ca}^{2+}$  transients from other studies<sup>[16-23]</sup>. Under the same UV-exposure condition, the neuronal electrical activity in the Mag-AS network was suppressed at first, and subsequently showed repeated synchronized activity. This result suggests the release of a neurohumoral factors from the Mag-AS, which suppressed excitation of neuronal activity. In fact, astrocytic  $\text{Ca}^{2+}$  activity associated with ATP release causes a decrease in the number of neuronal  $\text{Ca}^{2+}$  spikes<sup>[16-23]</sup>. In contrast, the glutamate, which induces astrocytic  $\text{Ca}^{2+}$  transients, is released near the synaptic connections during synchronized bursting activity, which

Formatted: Superscript

Formatted: Superscript

involves the N-methyl-D-aspartate glutamate receptor<sup>[16-23]</sup>. Therefore, our results suggest that neuronal activities also stimulated the astrocytes via a feedback loop-like electro-chemical interaction.

Formatted: Superscript

Our findings confirm that the astrocytic integration on a neuronal network was an effective method for neuronal modulation. Recent research on cell transplantation reported the production of dopaminergic and motor neurons from pluripotent stem cells ~~have been reported~~ for the treatment of neurological disorders<sup>[31, 32]</sup>. This method of neural transplantation is aimed at regrowing neurons in the damaged region. ~~In contrast, astrocytic transplantation has the potential to modulate the neural functions through the synaptic transmission by neurohumoral factors. Astrocytes, which enclose the circumference of a neuron, are widely distributed over the central and peripheral nervous system, so that access to the target sites may be relatively easy. However, it is also necessary to prevent unpleasant neuronal modulation by the functional control of astrocytes.~~ We expect our *in vitro* ~~vertically-layered~~ 3D co-culture method to further contribute to the ~~further~~ advancement of cell transplantation by providing basic research and safety assessment before the transplanting ~~the~~ astrocytes ~~to~~ *in vivo* in the nervous system.

Formatted: Superscript

Formatted: Font color: Red

## 5 Conclusions

Formatted: Font: Bold

We developed a method of MNP-injected astrocytes and magnetic force-based ~~vertically-layered~~ 3D co-culture for rapid and local integration of high-density astrocytes to neuronal networks. Extracellular recordings of electrical activity revealed that the network-wide neuronal activity was dynamically modulated by the astrocytic integration and Ca<sup>2+</sup> activation, and that astrocyte-induced neuronal activity generated ~~the~~ periodic synchronized bursting patterns. These results indicate that the astrocytic network manifests neuromodulatory functions possibly by using neurohumoral factors. Clarification of these mechanisms and their functional control method may contribute to astrocytic transplantation therapy.

Formatted: Font color: Red

Formatted: Font: Bold

## References

Formatted: Font: Bold, No underline

- 1 J. J. Pancrazio, E. W. Keefer, W. Ma, D. A. Stenger, and G. W. Gross, *Neurotoxicology*, 2001, **22**, 393-400.
- 2 G. Xiang, L. Pan, L. Huang, Z. Yu, X. Song, J. Cheng, W. Xing, and Y. Zhou, *Biosens. Bioelectron.*, 2007, **15**, 2478-2484.

- 3 [S. Illes, W. Fleischer, M. Siebler, H. P. Hartung, and M. Dihn , \*Exp. Neurol.\*, 2007, \*\*207\*\*, 171-176.](#)
- 4 [M. Chiappalone, A. Vato, L. Berdondini, M. Koudelka-Hep, and S. Martinoia, \*Int. J. Neural Syst.\*, 2007, \*\*17\*\*, 87-103.](#)
- 5 [A. Saito, Y. Takayama, H. Moriguchi, K. Kotani, and Y. Jimbo, \*IEEE Trans. Biomed. Eng.\*, 2014, \*\*61\*\*, 463-472.](#)
- 6 [Y. Jimbo, T. Tateno, and H. P. Robinson, \*Biophys. J.\*, 1999, \*\*76\*\*, 670-678.](#)
- 7 [G. Shahaf and S. Marom, \*J. Neurosci.\*, 2001, \*\*21\*\*, 8782-8788.](#)
- 8 [D. A. Wagenaar, R. Madhavan, J. Pine and S. M. Potter, \*J. Neurosci.\*, 2005, \*\*5\*\*, 680-688.](#)
- 9 [H. A. Johnson, A. Goel, and D. V. Buonomano, \*Nat. Neurosci.\*, 2010, \*\*13\*\*, 917-919.](#)
- 10 [J. F. Meyer, B. Wolf, and G. W. Gross, \*IEEE Trans. Biomed. Eng.\*, 2009, \*\*56\*\*, 1512-1523.](#)
- 11 [H. Takahashi, T. Sakurai, H. Sakai, D. J. Bakkum, J. Suzurikawa, R. Kanzaki R, \*Biosystems\*, 2012, \*\*107\*\*, 106-112.](#)
- 12 [A. M. Taylor, M. Blurton-Jones, S. W. Rhee, D. H. Cribbs, C. W. Cotman, and N. L. Jeon, \*Nat. Methods\*, 2005, \*\*2\*\*, 599-605.](#)
- 13 [J. Park, H. Koito, J. Li, and A. Han, \*Lab Chip\*, 2012, \*\*12\*\*, 3296-3304.](#)
- 14 [A. Takeuchi, S. Nakafutami, H. Tani, M. Mori, Y. Takayama, H. Moriguchi, K. Kotani, K. Miwa, J. K. Lee, M. Noshiro, Y. Jimbo, \*Lab Chip\*, 2011, \*\*11\*\*, 2268-2275.](#)
- 15 [Y. Takayama, H. Moriguchi, K. Kotani, T. Suzuki, K. Mabuchi, and Y. Jimbo, \*Biosystems\*, 2011, \*\*107\*\*, 1-8.](#)
- 16 [P. G. Haydon, \*Nat. Rev. Neurosci.\*, 2001, \*\*2\*\*, 185-193.](#)
- 17 [E. A. Newman, \*Trends Neurosci.\*, 2003, \*\*26\*\*, 536-542.](#)
- 18 [S. Koizumi, K. Fujishita, M. Tsuda, Y. Shigemoto-Mogami, and K. Inoue, \*Proc. Natl. Acad. Sci. USA\*, 2003, \*\*100\*\*, 11023-11028.](#)
- 19 [T. Fellin, O. Pascual, S. Gobbo, T. Pozzan, P. G. Haydon, and G. Carmignoto, \*Neuron\*, 2004, \*\*43\*\*, 729-743.](#)
- 20 [E. Scemes and C. Giaume, \*Glia\*, 2006, \*\*57\*\*, 716-725.](#)
- 21 [T. Fellin, \*J. Neurochem.\*, 2009, \*\*108\*\*, 533-544.](#)
- 22 [G. Christian, K. Annette, R. Lisa, H. David, and R. Nathalie, \*Nat. Rev. Neurosci.\*, 2010, \*\*11\*\*, 87-99.](#)
- 23 [P. Ulrike, V. Lydia, R. J rger, E. Pascal, H. David, G. Christian, and S. Eva, \*Proc. Natl. Acad. Sci. USA\*, 2011, \*\*108\*\*, 8467-8472.](#)
- 24 [T. Sasaki, N. Matsuki, and Y. Ikegaya, \*Science\*, 2011, \*\*331\*\*, 599-601.](#)
- 25 [G. F. Tian, H. Azmi, T. Takano, Q. Xu, W. Peng, J. Lin, N. Oberheim, N. Lou, X. Wang, H. R. Zielke, J. Kang, M. Nedergaard, \*Nat. Med.\*, 2005, \*\*11\*\*, 973-981.](#)
- 26 [L. H ja, \*Curr. Med. Chem.\*, 2014, \*\*21\*\*, 755-763.](#)

- [27 M. Nedergaard, B. Ransom, and S. A. Goldman, \*Trends Neurosci.\*, 2003, \*\*26\*\*, 523-530.](#)
- [28 K. Shimizu, A. Ito, J. K. Lee, T. Yoshida, K. Miwa, H. Ishiguro, Y. Numaguchi, T. Murohara, I. Kodama, and H. Honda, \*Biotechnol. Bioeng.\*, 2007, \*\*96\*\*, 803-809.](#)
- [29 H. Hama, C. Hara, K. Yamaguchi, and A. Miyawaki, \*Neuron\*, 2004, \*\*41\*\*, 405-415.](#)
- [30 M. D. Boehler, B. C. Wheeler, and G. J. Brewer, \*Neuron Glia Biol.\*, 2007, \*\*3\*\*, 127-140.](#)
- [31 S. Kriks, J. W. Shim, J. Piao, Y. M. Ganat, D. R. Wakeman, Z. Xie, L. Carrillo-Reid, G. Auyeung, C. Antonacci, A. Buch, L. Yang, M. F. Beal, D. J. Surmeier, J. H. Kordower, V. Tabar, and L. Studer, \*Nature\*, 2011, \*\*480\*\*, 47-551.](#)
- [32 M. Nakamura, and H. Okano, \*Cell Res.\*, 2013, \*\*23\*\*, 70-80.](#)

- [1] J. J. Panerazio, E. W. Keefer, W. Ma, D. A. Stenger, and G. W. Gross, "Neurophysiologic effects of chemical agent hydrolysis products on cortical neurons in vitro", *Nurotoxicology*, vol. 22, no. 3, pp. 393-400, 2001.
- [2] G. Xiang, L. Pan, L. Huang, Z. Yu, X. Song, J. Cheng, W. Xing, and Y. Zhou, "Microelectrode array-based system for neuropharmacological applications with cortical neurons cultured in vitro", *Bisens Bioelectron*, vol. 15, no. 11, pp. 2478-2484, 2007.
- [3] S. Illes, W. Fleischer, M. Siebler, H. P. Hartung, and M. Dihn e, "Development and pharmacological modulation of embryonic stem cell derived neuronal network activity", *Exp Neurol*, vol. 207, no. 1, pp. 171-176, 2007.
- [4] M. Chiappalone, A. Vato, L. Berdondini, M. Koudelka-Hep, and S. Martinoia, "Network dynamics and synchronous activity in cultured cortical neurons", *Int J Neural Syst*, vol. 17, no. 2, pp. 87-103, 2007.
- [5] A. Saito, Y. Takayama, H. Moriguchi, K. Kotani, and Y. Jimbo, "Induced Current-Pharmacological Split Stimulation System for Neuronal Networks", *IEEE Trans Biomed Eng.*, vol. 61, no. 2, pp. 463-472, 2014.
- [6] Y. Jimbo, T. Tateno, and H. P. Robinson, "Simultaneous induction of pathway-specific potentiation and depression in networks of cortical neurons", *Biophys J*, vol. 76, no. 2, pp. 670-678, 1999.

- [7] G. Shahaf and S. Marom, "Learning in networks of cortical neurons", *J Neurosci*, vol. 21, no. 22, pp. 8782-8788, 2001.
- [8] D. A. Wagenaar, R. Madhavan, J. Pine and S. M. Potter, "Controlling bursting in cortical cultures with closed-loop multi-electrode stimulation", *J Neurosci*, vol. 5, no. 3, pp. 680-688, 2005.
- [9] H. A. Johnson, A. Goel, and D. V. Buonomano, "Neural dynamics of in vitro cortical networks reflects experienced temporal patterns", *Nat Neurosci*, vol. 13, no. 8, pp. 917-919, 2010.
- [10] — J. F. Meyer, B. Wolf, and G. W. Gross, "Magnetic stimulation and depression of mammalian networks in primary neuronal cell cultures", *IEEE Trans Biomed Eng.*, vol. 56, no. 5, pp. 1512-1523, 2009.
- [11] — H. Takahashi, T. Sakurai, H. Sakai, D. J. Bakkum, J. Suzurikawa, R. Kanzaki R, "Light-addressed single-neuron stimulation in dissociated neuronal cultures with sparse expression of ChR2", *Biosystems*, vol. 107, no. 2, pp. 106-112, 2012.
- [12] — A. M. Taylor, M. Blurton-Jones, S. W. Rhee, D. H. Cribbs, C. W. Cotman, and N. L. Jeon, "A microfluidic culture platform for CNS axonal injury, regeneration and transport", *Nat Methods*, vol. 2, no. 8, pp. 599-605, 2005.
- [13] — J. Park, H. Koito, J. Li, and A. Han, "Multi-compartment neuron-glia co-culture platform for localized CNS axon-glia interaction study", *Lab Chip*, vol. 12, no. 18, pp. 3296-3304, 2012.
- [14] — A. Takeuchi, S. Nakafutami, H. Tani, M. Mori, Y. Takayama, H. Moriguchi, K. Kotani, K. Miwa, J. K. Lee, M. Noshiro, Y. Jimbo, "Device for co-culture of sympathetic neurons and cardiomyocytes using microfabrication", vol. 11, no. 13, 2011.
- [15] — Y. Takayama, H. Moriguchi, K. Kotani, T. Suzuki, K. Mabuchi, and Y. Jimbo, "Network-wide integration of stem cell-derived neurons and mouse cortical neurons using microfabricated co-culture devices", *Biosystems*, vol. 107, no. 1, pp. 1-8, 2011.
- [16] — P. G. Haydon, "GLIA: listening and talking to the synapse", *Nat Rev Neurosci*, vol. 2, no. 3, pp. 185-193, 2001.
- [17] — E. A. Newman, "New roles for astrocytes: regulation of synaptic transmission", *Trends Neurosci.*, vol. 26, no. 10, pp. 536-542, 2003.
- [18] — S. Koizumi, K. Fujishita, M. Tsuda, Y. Shigemoto-Mogami, and K. Inoue, "Dynamic inhibition of excitatory synaptic transmission by astrocyte-derived ATP in hippocampal cultures", *Proc Natl Acad Sci USA*, vol. 100, no. 19, pp. 11023-11028, 2003.
- [19] — T. Fellin, O. Pascual, S. Gobbo, T. Pozzan, P. G. Haydon, and G. Carmignoto,

- “Neuronal synchrony mediated by astrocytic glutamate through activation of extrasynaptic NMDA receptors”, *Neuron*, vol. 43, no. 5, pp. 729-743, 2004.
- [20] — E. Seemee and C. Giaume, “Astrocyte calcium waves: What they are and what they do”, *Glia*, vol. 57, no. 7, pp. 716-725, 2006.
- [21] — T. Fellin, “Communication between neurons and astrocytes: relevance to the modulation of synaptic and network activity”, *J Neurochem*, vol. 108, no. 3, pp. 533-544, 2009.
- [22] — G. Christian, K. Annette, R. Lisa, H. David, and R. Nathalie, “Astroglial networks: a step further in neuroglial and gliovascular interactions”, *Nat Rev Neurosci*, vol. 11, no. 2, pp. 87-99, 2010.
- [23] — P. Ulrike, V. Lydia, R. Jürgen, E. Pascal, H. David, G. Christian, and S. Eva, “Astroglial networks scale synaptic activity and plasticity”, *Proc Natl Acad of Sci USA*, vol. 108, no. 20, pp. 8467-8472, 2011.
- [24] — T. Sasaki, N. Matsuki, and Y. Ikegaya, “Action-Potential Modulation During Axonal Conduction”, *Science*, vol. 331, no. 6017, pp. 599-601, 2011.
- [25] — G. F. Tian, H. Azmi, T. Takano, Q. Xu, W. Peng, J. Lin, N. Oberheim, N. Lou, X. Wang, H. R. Zielke, J. Kang, M. Nedergaard: “An astrocytic basis of epilepsy”, *Nat Med*, vol. 11, no. 9, pp. 973-981, 2005.
- [26] — L. Héja, “Astrocytic target mechanisms in epilepsy”, *Curr Med Chem*, vol. 21, no. 6, pp. 755-763, 2014
- [27] — M. Nedergaard, B. Ransom, and S. A. Goldman, “New roles for astrocytes: redefining the functional architecture of the brain”, *Trends Neurosci*, vol. 26, no. 10, pp. 523-530, 2003.
- [28] — K. Shimizu, A. Ito, J. K. Lee, T. Yoshida, K. Miwa, H. Ishiguro, Y. Numaguchi, T. Murohara, I. Kodama, and H. Honda, “Construction of multi-layered cardiomyocyte sheets using magnetite nanoparticles and magnetic force”, *Biotechnol Bioeng*, Vol. 96, pp. 803-809, 2007.
- [29] — H. Hama, C. Hara, K. Yamaguchi, and A. Miyawaki, “PKC Signaling Mediates Global Enhancement of Excitatory Synaptogenesis in Neurons Triggered by Local Contact with Astrocytes”, *Neuron*, vol. 41, no. 3, pp. 405-415, 2004.
- [30] — M. D. Boehler, B. C. Wheeler, and G. J. Brewer, “Added astroglia promote greater synapse density and higher activity in neuronal networks”, *Neuron-Glia Biol*, vol. 3, no. 2, pp. 127-140, 2007.
- [31] — S. Kriks, J. W. Shim, J. Piao, Y. M. Ganat, D. R. Wakeman, Z. Xie, L. Carrillo-Reid, G. Auyeung, C. Antonacci, A. Buch, L. Yang, M. F. Beal, D. J. Surmeier, J. H. Kordower, V. Tabar, and L. Studer, “Dopamine neurons derived from

human ES cells efficiently engraft in animal models of Parkinson's disease", vol. 480, no. 7378, pp. 47-551, 2011.

[32] — M. Nakamura, and H. Okano, "Cell transplantation therapies for spinal cord injury focusing on induced pluripotent stem cells", *Cell Res*, vol. 23, no. 1, pp. 70-80, 2013.

[33] — T. Kondo, M. Funayama, K. Tsukita, A. Hotta, A. Yasuda, S. Nori, S. Kaneko, M. Nakamura, R. Takahashi, H. Okano, S. Yamanaka, and H. Inoue, "Focal transplantation of human iPSC-derived glial-rich neural progenitors improves lifespan of ALS mice", *Stem Cell Reports*, vol. 3, no.2, pp. 242-249, 2014.

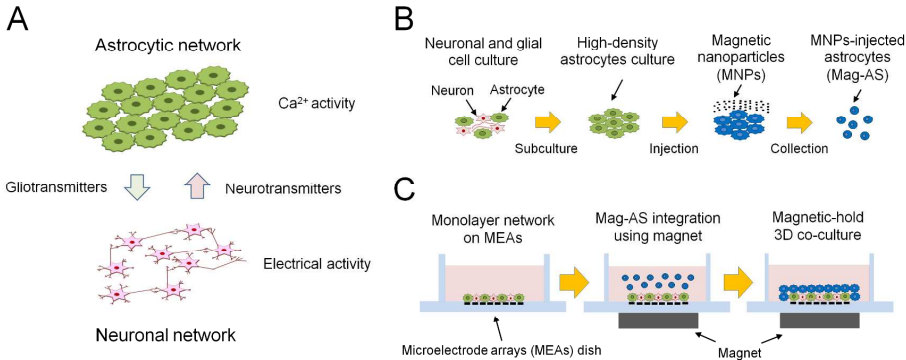


Fig. 1. Schematic view of the principle and method of vertically-layered 3D astrocytic network integration on the monolayer neuronal culture. (A) Electrical and chemical activity-dependent interaction between neuronal and astrocytic network. Neurotransmitters are released with neuronal electrical activity and gliotransmitters are released with astrocytic  $Ca^{2+}$  oscillations. The different chemical agents are mutually dependent. (B) Selective culture of high-density astrocytes for preparation of MNP-injected astrocytes (Mag-AS). Neuronal cells are killed by repeated subculture. After confluent growth during long-term culture, astrocytes are used in the MNP-injection

Formatted: Font: (Default) Times New Roman

Formatted: Font: (Default) Times New Roman, Font color: Red

Formatted: Font: (Default) Times New Roman

experiments. (C) Vertically-layered 3D co-culture method using external magnetic force fields and electrical activity recording from MEA. Monolayer neuronal and astrocytic networks are cultured on MEA. After maturation of spontaneous electrical activities, the monolayer networks are covered with Mag-AS by using magnetic force.

Formatted: Font: (Default) Times New Roman, Font color: Red

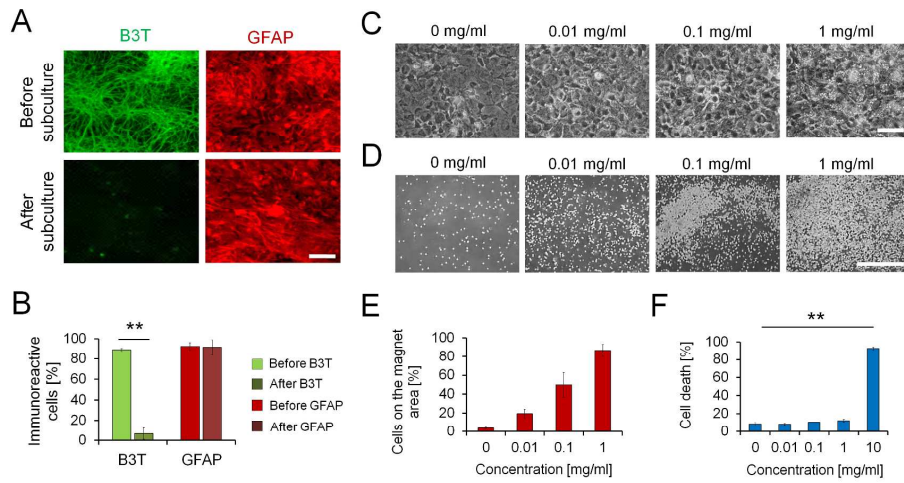
Formatted: Font: (Default) Times New Roman

Formatted: Font: (Default) Times New Roman, Font color: Red

Formatted: Font: (Default) Times New Roman

Formatted: Font: (Default) Times New Roman, Font color: Red

Formatted: Font: (Default) Times New Roman





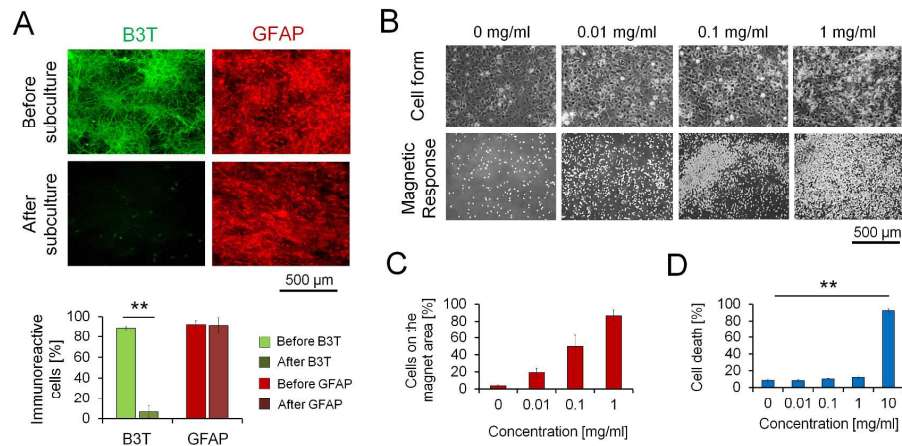


Fig. 2. Results of selective culture, magnetic responses and cell death analysis after injection of the MNPs into astrocytes. (A) Immunohistochemical images Assessment of neuronal and glial cells death after subculture with immunohistochemical analysis. (B) The percentage of beta-III tubulin (B3T) positive neurons decreased by 82.2% after repeated subculture, but no reduction of glial fibrillary acidic protein (GFAP) positive cells was not observed in the same samples. (C) Phase contrast images of cell morphology after MNP injection. Astrocytes were markedly covered with MNPs at concentration of 1 mg/mL. (D) Magnetic response of MNP-injected astrocytes (Mag-AS). The magnetic responses increased linearly with concentrations of 0, 0.01, 0.1, and 1 mg/mL. (E) Cell death analysis related to MNP concentration. Morphological changes were not seen in after MNP injection of astrocytes. The magnetic responses increased linearly with concentrations of 0, 0.01, 0.1, and 1 mg/mL. The percentage of cell death did not change with these concentrations; however, significant cell death was observed at the control concentration of 10 mg/mL (\*\* $P < 0.001$ ,  $n = 4$ , error bars  $\pm$ SD).

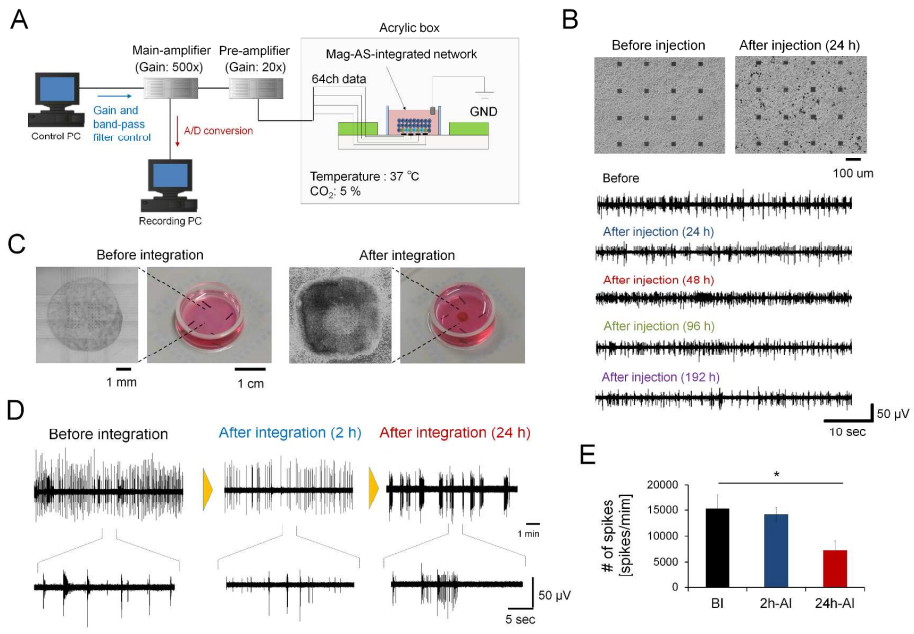
Formatted: Font color: Red

Formatted: Font color: Red

Formatted: Font color: Red

Formatted: Font color: Red

Formatted: Font color: Red



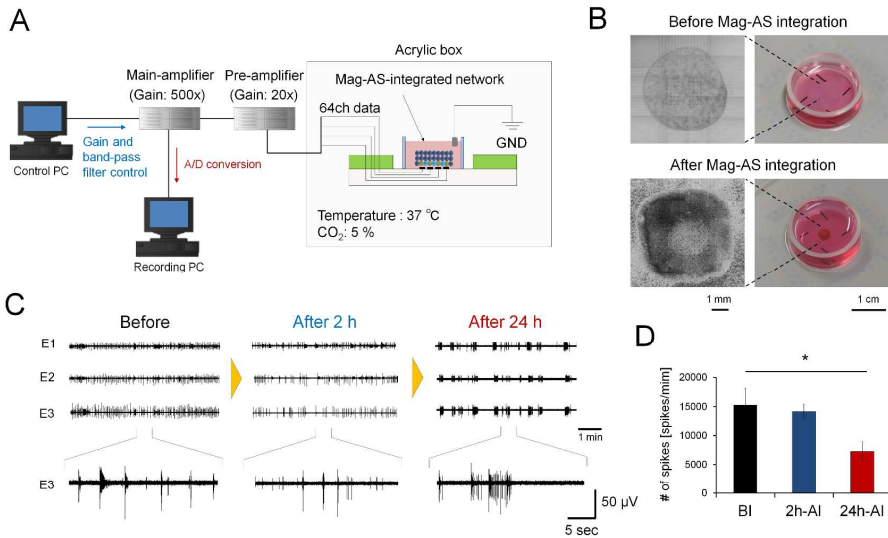


**Fig. 3.** Modulation of neuronal electrical activity by Mag-AS integration. **(A)** Schematic diagram of extracellular recording system to evaluate the spatiotemporal patterns of spontaneous activity during integration of Mag-AS. **(B)** Time-dependent changes of spontaneous activities in monolayer network after MNP injection. **(C)** Morphological changes of cultured neuronal networks after Mag-AS integration. Magnetically collected astrocytes are holding regionally onto the MEA-attached monolayer neuronal and astrocytic networks. Time-dependent changes of **(D)** spontaneous electrical activity patterns and **(E)** number of spikes before integration (BI) and after integration (AI) of Mag-AS. The multi-site recording data show that Mag-AS integration induced widely synchronized activity after 24 h. On the other hand, the number of spikes was reduced 24 h after integration of Mag-AS ( $*P < 0.05$ ,  $n = 6$ , error bars  $\pm$ SD).

Formatted: Font: (Default) Times New Roman

Formatted: Font: (Default) Times New Roman, Font color: Red

Formatted: Font: (Default) Times New Roman

Formatted: Font: (Default) Times New Roman, Font color: Red

Formatted: Font: (Default) Times New Roman

Formatted: Font: (Default) Times New Roman, Font color: Red

Formatted: Font: (Default) Times New Roman

Formatted: Font: (Default) Times New Roman, Font color: Red

Formatted: Font: (Default) Times New Roman

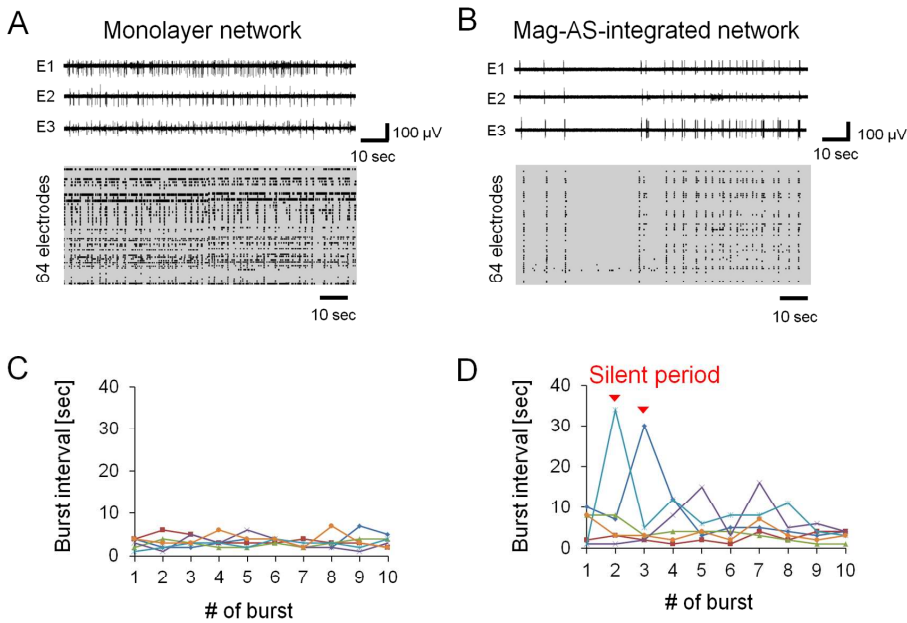
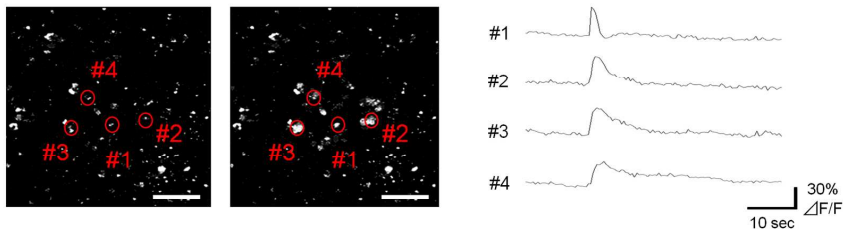


**Fig. 4.** Silent periods were observed in Mag-AS-integrated neuronal and astrocytic networks. Typical results of raster plot analysis of (A) monolayer and (B) Mag-AS-integrated network activity. Samples of Mag-AS-integrated network activity were obtained after 24 h integration. These recordings show widely synchronized spontaneous activity, and Mag-AS-integrated networks occasionally paused their activity for certain (silent) periods. Temporal properties of (C) monolayer and (D) Mag-AS-integrated networks are inspected by measuring the time intervals of synchronized bursting activities. Generally, the bursting intervals of monolayer networks were shorter than 10 s, while bursting intervals longer than 20–30 s were observed in the Mag-AS-integrated network.

Formatted: Font: (Default) Times New Roman

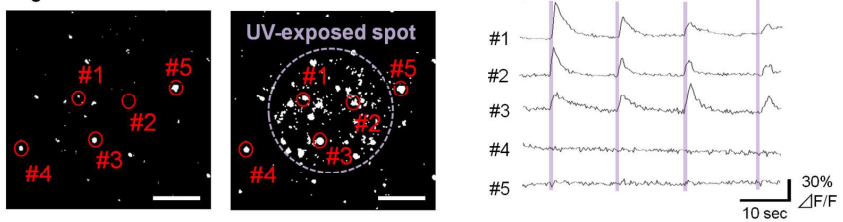
A

Spontaneous calcium transients

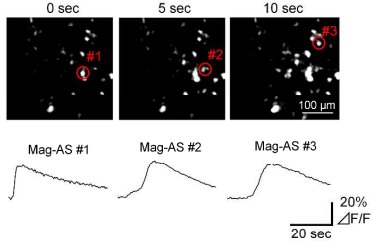


B

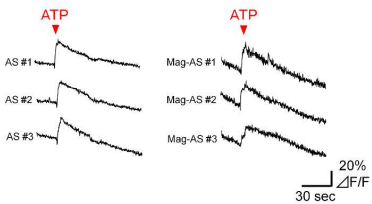
Caged calcium-induced calcium transients



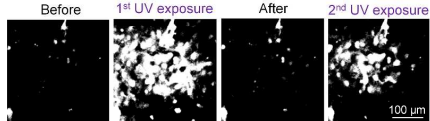
A



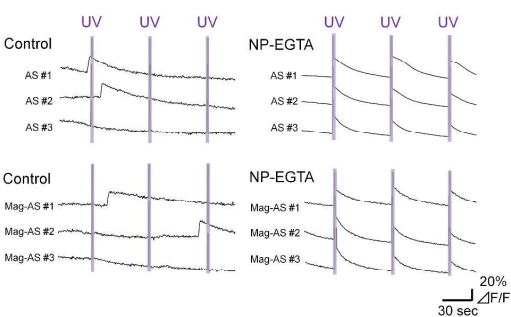
B



C



D



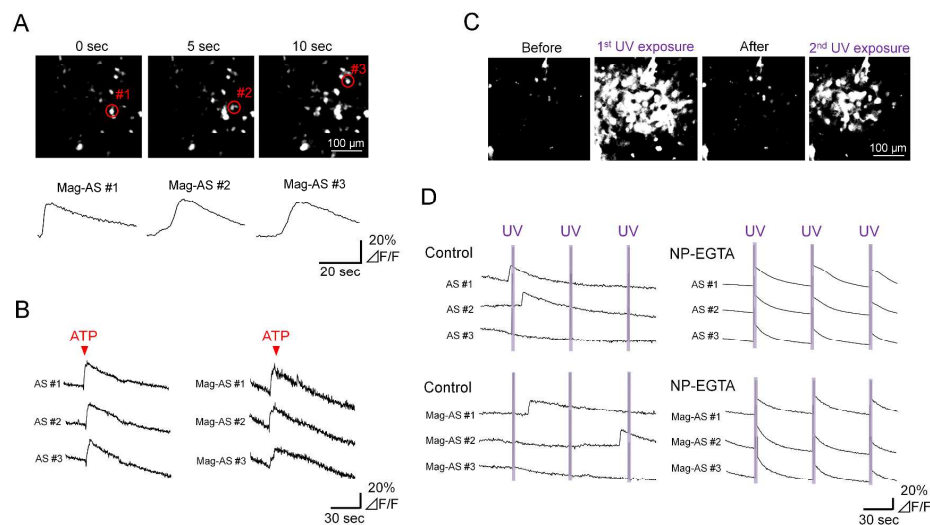


**Fig. 5.** Spontaneous and artificial increase of intracellular  $\text{Ca}^{2+}$  concentration of Mag-AS-integrated networks. (A) Spontaneous and wave-like  $\text{Ca}^{2+}$  transients in the Mag-AS network. Spontaneous  $\text{Ca}^{2+}$  uptake is initiated by an astrocyte (#1) and activation spreads to the surrounding astrocytes (#2 and #3). (B) ATP responses of monolayer astrocytes and Mag-AS. Astrocytes respond to ATP even after MNP injection. (C) Artificial simultaneous  $\text{Ca}^{2+}$  release of Mag-AS using caged calcium (NP-EGTA AM) and localized UV exposure. The caged calcium was only activated during the UV-exposed period of Mag-AS. Although the astrocytes had a widely-respondered widely to repetitive stimulation, the rise of calcium concentration in the UV-exposed area was gradually decreased. (D) The effects of UV exposure on caged- or uncaged-monolayer and MNP-injected astrocytes. Changes of astrocytic excitation were not seen in a UV exposure only. Rapid upregulation of intracellular  $\text{Ca}^{2+}$  transients by NP-EGTA AM occurred concurrently with UV exposure. These features were similarly seen in the monolayer and MNP-injected astrocytes, and the induced waveforms were similar to the spontaneous wave-like  $\text{Ca}^{2+}$  transients.

Formatted: Font: (Default) Times New Roman

Formatted: Font: (Default) Times New Roman, Font color: Red

Formatted: Font: (Default) Times New Roman

Formatted: Font: (Default) Times New Roman, Font color: Red

Formatted: Font: (Default) Times New Roman

Formatted: Font: (Default) Times New Roman, Font color: Red

Formatted: Font: (Default) Times New Roman

Formatted: Font: (Default) Times New Roman, Font color: Red

Formatted: Font: (Default) Times New Roman, Font color: Red

Formatted: Font: (Default) Times New Roman, Font color: Red

Formatted: Font: (Default) Times New Roman

Formatted: Font: (Default) Times New Roman, Font color: Red

Formatted: Font: (Default) Times New Roman, Font color: Red

Formatted: Font: (Default) Times New Roman, Font color: Red

Formatted: Font: (Default) Times New Roman, Font color: Red

Formatted: Font: (Default) Times New Roman, Font color: Red

Formatted: Font: (Default) Times New Roman, Font color: Red

Formatted: Font: (Default) Times New Roman, Font color: Red

Formatted: Font: (Default) Times New Roman, Font color: Red

Formatted: Font: (Default) Times New Roman, Font color: Red

Formatted: Font: (Default) Times New Roman, Font color: Red, Superscript

Formatted: Font: (Default) Times New Roman, Font color: Red

Formatted: Font: (Default) Times New Roman, Font color: Red

Formatted: Font: (Default) Times New Roman, Font color: Red

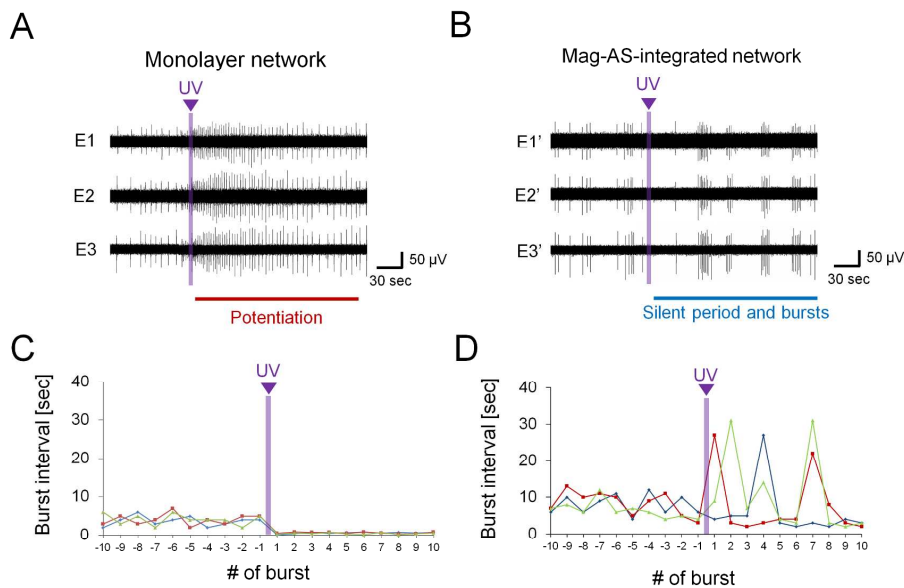


**Fig. 6.** Real-time detection of neuronal network activity modulation by activation of integrated Mag-AS. Release of caged calcium triggered the modulation of ~~the~~ spontaneous activity patterns of (A) monolayer and (B) Mag-AS-integrated networks. The caged calcium-evoked responses were reversed by the Mag-AS integration. While the spontaneous electrical activity in the monolayer networks was enhanced by the release of caged calcium, a suppressive effect was observed in the Mag-AS-integrated networks. The time interval of synchronized bursting clearly differed between (C) monolayer ( $n = 3$ ) and (D) Mag-AS-integrated networks ( $n = 3$ ), indicating the generation of silent periods with activation of the Mag-AS network.

Formatted: Font: (Default) Times New Roman

|

